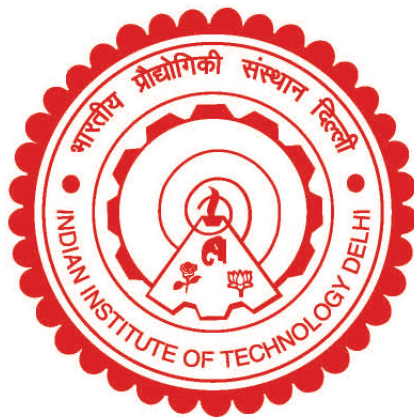


A THERMO-ELECTROCHEMICAL INVESTIGATION OF LITHIUM-ION BATTERIES

ROHIT MEHTA



**DEPARTMENT OF MECHANICAL ENGINEERING
INDIAN INSTITUTE OF TECHNOLOGY DELHI**

April, 2023

A THERMO-ELECTROCHEMICAL INVESTIGATION OF LITHIUM-ION BATTERIES

by

ROHIT MEHTA

submitted

in fulfillment of the requirements of the degree of

Doctor of Philosophy

to the



**DEPARTMENT OF MECHANICAL ENGINEERING
INDIAN INSTITUTE OF TECHNOLOGY DELHI**

April, 2023

© Indian Institute of Technology Delhi (IITD), New Delhi, 2022

I would like to dedicate this thesis to my loving family . . .

CERTIFICATE

This is to certify that the thesis entitled "A **thermo-electrochemical investigation of lithium-ion batteries**" being submitted by **Mr. Rohit Mehta** to the **Indian Institute of Technology Delhi** for the award of the degree of **Doctor of Philosophy** is a bonafide record of original research work carried out by him under our supervision in conformity with rules and regulations of the institute. The results presented in this thesis have not been submitted, in part or in full, to any other University or Institute for the award of any degree or diploma.

Dr. Amit Gupta

Professor

Department of Mechanical Engineering,

Indian Institute of Technology Delhi,

New Delhi-110016, India.

ACKNOWLEDGEMENTS

I would like to express my sincere gratitude to my supervisor, **Dr. Amit Gupta**, for his invaluable guidance and support. His intellectual counsel and suggestions during the various stages of my PhD was the backbone that paved way to deliver my best and accomplish the desired objectives. It was a great privilege to work with him. I always enjoyed discussions with him. He gave me motivational support throughout my research work at IIT Delhi.

I wish to thank my dissertation committee members, **Dr. M.R. Ravi**, **Dr. Supreet Singh Bahga** and **Dr. Anil Verma**, for their positive criticism and valuable comments while evaluating my research plan, progress and synopsis of my dissertation. Their valuable suggestions helped me improve my work.

I also wish to thank **Dr. Amit Gupta**, **Dr. Supreet Singh Bahga**, **Dr. Shubhendu Bhasin** and Anirudh Nath for their fruitful inputs and discussions while working under the DST sponsored project. I am grateful for the knowledge of controls and observer designs gained during this period.

I am thankful to my colleagues at the TESLA for creating a vibrant atmosphere in the lab. A special thanks to Salahuddin Ahamad, Raghvendra Gupta and Mayur Gaikwad for their support and fruitful discussions in the field of lithium-ion research. I am grateful for the practical knowledge and experience shared by Salahuddin Ahamad and Mayur Gaikwad. The contribution of Raghvendra Gupta in performing experiments was of immense value. I am also thankful for the companionship of Parvez Ahamad and Binoy Bhargwan during my research. I am grateful to Ashish Joshi and Sumona for allowing access to their lab equipments in the Textile department.

I also appreciate and cherish the friendship of Ajay Lodhi and Gaurav Nath that helped me enjoy the life at IIT Delhi beyond my doctoral research work.

I am grateful to my parents, brother, and extended family for their unconditional love and unwavering support without which this work would not have reached its final form.

Rohit Mehta

ABSTRACT

The primary concern associated with lithium-ion batteries is safety during high-power utilization. Being able to estimate the internal states of the battery accurately in real-time is essential to prevent unsafe operating conditions. Furthermore, understanding the heat generation phenomenon during the cycling of cells is required as using these cells in fast-charging and high-power applications will become ubiquitous as the world shifts towards renewable energy generation. Towards this goal, the present study proposes a reduced-order electrochemical model that can be implemented for state estimation in real-time algorithms. Moreover, the heat of mixing in lithium-ion cells is modelled using a volume-averaged local thermal model, and its significance towards heat generation in lithium-ion cells is analyzed. Lastly, the proposed thermo-electrochemical model is simulated to predict the temperature of cylindrical lithium-ion cells. Its results are validated against experimental data. Various parameters required in the thermal and electrochemical models are experimentally determined.

Reduced-order physics-based models can achieve accurate state estimation due to the implementation of the inherent physics while remaining computationally inexpensive to be applied in real-time estimation-based algorithms. Towards this goal, a polynomial-based isothermal reduced order model is proposed in this work. This model can account for the spatial and temporal dynamics of the electrodes and the electrolyte. A novel approach is developed to account for the spatially varying overpotential and open-circuit potential. Moreover, we employ a semi-analytical model for lithium diffusion in the electrode and exhibit that it can provide great flexibility between accuracy and computational cost. We provide a criterion for truncating the semi-analytical solution to achieve high accuracy under fluctuating current applications based on the electrodes' characteristic diffusion time scale. A comparative analysis performed with an existing reduced-order polynomial model demonstrates that our model reduces error by a factor of five during cell voltage prediction for currents as high as $7C$. The performance of our

model is also presented under dynamic test conditions like US06 and FTP75 drive cycles. The computational time taken by our solver is close to the single-particle model despite incorporating electrolyte dynamics.

Moreover, we propose a local thermo-electrochemical pseudo-two-dimensional model accounting for the heat of mixing in the electrodes. Due to a lack of research towards the heat of mixing, the understanding of heat of mixing is fairly limited for lithium-ion cells. To the best of our knowledge, such a model has been implemented for the first time. The model is used to simulate, analyze and understand the temporal and spatial variation of heat generation in a lithium-ion cell. We show that the heat of mixing can contribute significantly towards the total heat generation in the cell under poor diffusion dynamics conditions and should be considered when developing a thermal model. In our simulations, the heat of mixing contributed as high as 9%-16% for 1C-5C discharge current and 38%-48% for 2C-5C charge current towards the total heat. In contrast to an earlier study, we show that it is not necessary for the contribution of the heat of mixing to increase with the current rate. Several sources like the ohmic heat, irreversible heat of reaction, and the heat of mixing increase with current, and the net interplay between these sources decide which component will become more significant at higher currents. Finally, a reduced-order formulation of this model is validated against the experimental cell voltage and temperature data for cylindrical cells. Experimental determination of several thermodynamical, electrochemical and geometrical model parameters is carried out. The dimensions of the cylindrical cell components are determined by disassembling the cell. Material characterization techniques, including scanning electron microscopy and energy-dispersive x-ray spectroscopy, are performed to determine the electrode composition and particle sizes. The galvanostatic intermittent titration technique is employed to obtain the diffusion coefficient of the electrode materials.

सार

लिथियम-आयन बैटरी से जुड़ी प्राथमिक चिंता उच्च-शक्ति उपयोग के दौरान सुरक्षा है। असुरक्षित परिचालन स्थितियों को रोकने के लिए वास्तविक समय में बैटरी की आंतरिक स्थिति का सटीक अनुमान लगाने में सक्षम होना आवश्यक है। इसके अलावा, बैटरी के चक्रण के दौरान गर्मी उत्पादन की घटना को समझना आवश्यक है क्योंकि तेजी से चार्जिंग और उच्च-शक्ति अनुप्रयोगों में इन बैटरियों का उपयोग सर्वव्यापी हो जाएगा जैसे दुनिया अक्षय ऊर्जा उत्पादन की ओर बढ़ रही है। इस लक्ष्य की ओर, वर्तमान अध्ययन एक कम-क्रम वाले इलेक्ट्रोकेमिकल मॉडल का प्रस्ताव करता है जिसे वास्तविक समय एल्गोरिदम में आंतरिक स्थिति के आकलन के लिए लागू किया जा सकता है। इसके अलावा, लिथियम-आयन बैटरी में मिश्रण की गर्मी को वॉल्यूम-औसत स्थानीय थर्मल मॉडल का उपयोग करके तैयार किया गया है, और लिथियम-आयन बैटरी में गर्मी पैदा करने के प्रति इसके महत्व का विश्लेषण किया गया है। अंत में, प्रस्तावित थर्मो-इलेक्ट्रोकेमिकल मॉडल को बेलनाकार लिथियम-आयन बैटरी के तापमान की पूर्व-सूचना प्राप्त करने के लिए सिम्युलेट किया गया है। इसके परिणाम प्रयोगात्मक डेटा के खिलाफ सत्यापित किए गये हैं। थर्मल और इलेक्ट्रोकेमिकल मॉडल में आवश्यक विभिन्न पैरामीटर प्रयोगात्मक रूप से निर्धारित किए गये हैं।

कम-क्रम भौतिकी-आधारित मॉडल अंतर्निहित भौतिकी के कार्यान्वयन के कारण सटीक स्थिति अनुमान प्राप्त कर सकते हैं जबकि वास्तविक समय अनुमान-आधारित एल्गोरिदम में लागू होने के लिए कम्प्यूटेशनल रूप से सस्ते हैं। इस लक्ष्य की ओर, इस काम में एक बहुपद-आधारित इज़ोटेर्मल कम ऑर्डर मॉडल प्रस्तावित है। यह मॉडल इलेक्ट्रोड और इलेक्ट्रोलाइट के स्थानिक और लौकिक गतिशीलता का हिसाब रख सकता है। स्थानिक रूप से भिन्न अति-विभव और ओपन-सर्किट विभव को ध्यान में रखते हुए एक उपन्यास दृष्टिकोण विकसित किया गया है। इसके अलावा, हम इलेक्ट्रोड में

लिथियम प्रसार के लिए एक अर्ध-विश्लेषणात्मक मॉडल का उपयोग करते हैं और प्रदर्शित करते हैं कि यह सटीकता और कम्प्यूटेशनल लागत के बीच महान लचीलापन प्रदान कर सकता है। हम इलेक्ट्रोड की विशेषता प्रसार समय पैमाने के आधार पर वर्तमान विद्युत प्रवाह में उतार-चढ़ाव के तहत उच्च सटीकता प्राप्त करने के लिए अर्ध-विश्लेषणात्मक समाधान को छोटा करने के लिए एक मानदंड प्रदान करते हैं। एक मौजूदा कम-क्रम बहुपद मॉडल के साथ किया गया एक तुलनात्मक विश्लेषण दर्शाता है कि हमारा मॉडल 7C तक की धाराओं के लिए बैटरी वोल्टेज भविष्यवाणी के दौरान त्रुटि को पांच गुना कम कर देता है। हमारे मॉडल का प्रदर्शन यूएस -06 और एफटीपी -75 ड्राइव साइकिल जैसी गतिशील परीक्षण स्थितियों के तहत भी प्रस्तुत किया गया है। हमारे सॉल्वर द्वारा लिया गया कम्प्यूटेशनल समय इलेक्ट्रोलाइट गतिकी को शामिल करने के बावजूद सिंगल-पार्टिकल मॉडल के करीब है।

इसके अलावा, हम इलेक्ट्रोड में मिश्रण की गर्मी के लिए एक स्थानीय थर्मो-इलेक्ट्रोकेमिकल छद्म-द्वि-आयामी मॉडल का प्रस्ताव करते हैं। मिश्रण की ऊष्मा के प्रति अनुसंधान की कमी के कारण, लिथियम-आयन बैटरी के लिए मिश्रण की ऊष्मा की समझ काफी सीमित है। हमारी जानकारी के अनुसार, ऐसा मॉडल पहली बार लागू किया गया है। मॉडल का उपयोग लिथियम-आयन बैटरी में गर्मी उत्पादन के अस्थायी और स्थानिक भिन्नता को अनुकरण, विश्लेषण और समझने के लिए किया जाता है। हम दिखाते हैं कि खराब प्रसार गतिकी परिस्थितियों में मिश्रण की गर्मी बैटरी में कुल गर्मी उत्पादन में महत्वपूर्ण योगदान दे सकती है और थर्मल मॉडल विकसित करते समय इस पर विचार किया जाना चाहिए। हमारे सिमुलेशन में, मिश्रण की गर्मी ने 1C-5C डिस्चार्ज विद्युत प्रवाह के लिए 9% -16% और कुल गर्मी की ओर 2C-5C चार्ज विद्युत प्रवाह के लिए 38% -48% का योगदान दिया। पहले के एक अध्ययन के विपरीत, हम दिखाते हैं कि वर्तमान विद्युत प्रवाह के साथ मिश्रण की गर्मी के योगदान में वृद्धि आवश्यक नहीं है। ओमिक गर्मी, प्रतिक्रिया की अपरिवर्तनीय गर्मी, और मिश्रण की गर्मी जैसे कई स्रोत विद्युत प्रवाह के साथ बढ़ते हैं, और इन स्रोतों के बीच नेट परस्पर क्रिया तय करते हैं कि उच्च धाराओं पर कौन सा घटक अधिक महत्वपूर्ण हो जाएगा। अंत में, बेलनाकार बैटरी के लिए प्रायोगिक बैटरी

वोल्टेज और तापमान डेटा के खिलाफ इस मॉडल का एक कम-क्रम सूत्रीकरण सत्यापित किया गया है। कई ऊष्मप्रवैगिकी, विद्युत रासायनिक और ज्यामितीय मॉडल मापदंडों का प्रायोगिक निर्धारण किया जाता है। बेलनाकार बैटरी घटकों के आयाम इसे अलग करके निर्धारित किए जाते हैं। इलेक्ट्रोड संरचना और कण आकार निर्धारित करने के लिए स्कैनिंग इलेक्ट्रॉन माइक्रोस्कोपी और ऊर्जा-फैलाने वाले एक्स-रे स्पेक्ट्रोस्कोपी सहित सामग्री लक्षण वर्णन तकनीकों का प्रदर्शन किया जाता है। इलेक्ट्रोड सामग्री के प्रसार गुणांक को प्राप्त करने के लिए गैल्वेनोस्टैटिक आंतरायिक अनुमापन तकनीक का इस्तेमाल किया गया है।

CONTENTS

CERTIFICATE	i
ACKNOWLEDGEMENTS	ii
ABSTRACT	iv
CONTENTS	ix
List of Figures	xii
List of Tables	xvi
Nomenclature	xvii
1 Introduction	1
1.1 Background	1
1.1.1 Batteries- an energy storage device	2
1.1.2 Historical development of batteries	3
1.1.3 Lithium-ion batteries	4
1.2 Motivation	8
1.3 Objectives	11
1.4 Outline of the thesis	12
2 Literature review	14
2.1 Introduction	14
2.2 Electrical Models	16
2.2.1 Integral-order ECMs	17
2.2.2 Fractional-order ECMs	18
2.3 Data-driven models	21

2.4	Electrochemical models	25
2.4.1	Pseudo-2D model	25
2.4.2	Single-particle model	25
2.4.3	Other reduced-order models	27
2.5	Thermal models	33
2.5.1	Total energy balance model	33
2.5.2	Local energy balance model	36
2.5.3	Other reduced order models	38
2.6	Degradation models	40
2.6.1	Electrolyte reduction at the negative electrode	41
2.7	Conclusions	46
3	An improved single-particle model with electrolyte dynamics for high-current applications	48
3.1	Introduction	48
3.2	Methodology	50
3.2.1	Model development	50
3.2.2	Model Summary	62
3.3	Results and discussion	63
3.3.1	Model validation	65
3.3.2	Accuracy of semi-analytical solution	66
3.3.3	Static discharge and charge test	67
3.3.4	Dynamic test	69
3.3.5	Model assessment	71
3.3.6	Comparative analysis of computational time	76
3.4	Conclusions	77
4	A thermo-electrochemical pseudo two-dimensional model for lithium-ion cells considering heat of mixing	79

4.1	Introduction	79
4.2	Methodology	81
4.2.1	Model formulation	81
4.2.2	Numerical methodology	85
4.3	Results and discussion	86
4.3.1	Model validation	88
4.3.2	Isothermal cycling of cell	89
4.3.3	Non-isothermal cycling of cell	98
4.4	Conclusions	101
5	Thermal modelling of cylindrical lithium-ion cells	102
5.1	Introduction	102
5.2	Methodology	103
5.2.1	Model formulation	103
5.2.2	Experimental study	103
5.3	Results and discussion	111
5.4	Conclusions	115
6	Conclusions and suggestions for future work	116
	References	121
	List of Publications	152
	Biodata of the Author	155

List of Figures

1.1	Schematic indicating the oxidation-reduction reactions at the two electrodes during discharge for a battery.	3
1.2	(a) Various applications of lithium-ion cells, and (b) energy density v/s specific energy plot for various battery chemistries.	5
1.3	Comparison of desired cell characteristics for various commercially available cathode materials.	6
1.4	Various form factors available in lithium-ion cells.	6
1.5	Schematic of a lithium-ion cell.	7
1.6	Mechanism of thermal runaway in a lithium-ion cell.	10
2.1	Classification of lithium-ion models.	15
2.2	a.) A lithium-ion schematic and its equivalent representations in (b.) pseudo-2D, (c.) single particle and (d.) equivalent hydraulic models.	26
2.3	(a) Single (above) and two (below) thermal-mass models and (b) a unit cell of the thermal circuit model employed for thermal analysis of lithium-ion cells. . .	37
2.4	Various degradation processes and their stress factors associated with lithium-ion cells	41
3.1	Schematic of the proposed reduced-order model.	49
3.2	Comparison of (a) surface concentration and (b) percentage error with respect to finite-volume method (FVM) with 100 grids for the negative electrode based on semi-analytical model with nine terms of series, FVM with 20 grids, second-degree and fourth-degree polynomial approximations.	65
3.3	Comparison of lithium concentration in the electrolyte for the polynomial model with P2D model for US06 drive cycle.	66

3.4	Effect of different number of truncation terms on the surface concentration prediction for the electrodes based on Eq.(3.73) for (a) 1C pulse ($D_{s,n} = 1 \times 10^{-14}$), (b) 3C pulse ($D_{s,n} = 1 \times 10^{-14}$), (c) 5C pulse ($D_{s,n} = 1 \times 10^{-14}$), (d) 3C pulse ($D_{s,n} = 3.9 \times 10^{-14}$), (e) 3C pulse ($D_{s,n} = 3 \times 10^{-15}$) and (f) 3C pulse ($D_{s,p} = 1 \times 10^{-13}$) discharge-charge pulse of 100 s each.	68
3.5	Plots for comparison of cell voltage for the proposed and P2D models at various C-rates during (a) discharge and (b) charge.	69
3.6	Plots for comparison of (a), (c) and (e) voltage for P2D, SPM, SPM2 and the proposed model and (b), (d) and (f) percentage error in voltage for SPM2 and the proposed model with respect to P2D at 1C, 3C and 5C-rates of discharge.	70
3.7	Simulation input current and corresponding output voltage and percentage error with respect to P2D for (a), (c) and (e) US06 and (b), (d) and (f) FTP75 dynamic tests.	72
3.8	Plots for comparison of combined value of overpotential and OCP for the two electrodes at discharge C-rates of 1C, 3C and 5C.	74
3.9	Plots for comparison of electrolyte potential drop across cell in the proposed model with the P2D for (a) 1C, (b) 3C and (c) 5C-rates of discharge.	75
4.1	Pseudo-2D representation of the lithium-ion cell.	81
4.2	Flowchart representing the methodology adopted for the solver.	87
4.3	Comparison of (a) cell voltage and (b) total heat generation rate obtained at 3C-current for our model with the results of Gu et al. for same input model parameters.	88
4.4	Variation in cell voltage and heat generation in the cell for (a) 1C and (b) 3C discharge followed by a rest of 800s.	90
4.5	Comparison of heat generated in the cell with and without heat of mixing included for various (a) discharge and (b) charge currents between 1C-5C.	90

4.6	Contribution of different heat generation components to the total heat generation in a cell over time for (a) 3C and (b) 5C discharge; and (c) 3C and (b) 5C charge currents.	91
4.7	Reversible entropic heat generated in the cell for C/5 (a) discharge and (b) charge current.	92
4.8	Comparison between the total enthalpic heat generated and the enthalpic heat generated due to reaction at the surface for (a) negative electrode and (b) positive electrode for 5C discharge current, and for (c) negative electrode and (d) positive electrode for 5C charge current.	93
4.9	Variation of the rate of the heat of mixing with characteristic diffusion time-scale of the (a) & (b) negative electrode and (c) & (d) positive electrode for different (a) & (c) discharge and (b) & (d) charge current conditions.	94
4.10	Spatial variation of the heat generation components with the thickness of the cell for 5C current at (a) 30s from beginning of discharge, (b) end of discharge, (c) 30s from beginning of charge and (d) end of charge.	96
4.11	Temporal variation of cell temperature with and without heat of mixing included for (a) 1C discharge, (b) 1C charge, (c) 3C discharge, (d) 3C charge, (e) 5C discharge and (f) 5C charge current.	97
5.1	(a) The experimental setup for cycling of the cell under controlled ambient temperature (the cell and cell holder within the thermal chamber are displayed in the inset), and the (a) view of a disassembled cell.	104
5.2	SEM images of (a) graphite and (b) NMC electrodes at 1500x magnification and (c) graphite and (d) NMC electrodes at 5000x magnification.	105
5.3	EDX spectrum of the NMC electrode.	106
5.4	Variation of cell's surface temperature during (a) 2C discharge-charge pulse test and (b) rest period after 1C discharge at SoC=0.5.	107

5.5	(a) Second derivative of the open circuit potential (OCP) for full and NMC half cells used for scaling and alignment, (b) OCP of the full cell and half cells against cell's SoC; and the OCP of (c) positive and (d) negative electrodes. . . .	109
5.6	(a) A pulse of the GITT test for NMC electrode and (b) variation in the diffusion coefficients of the two electrodes with cell SoC at 25°C.	110
5.7	Entropic heat coefficient for (a) graphite and (b) NMC electrodes.	111
5.8	Comparison between the experimentally and numerically obtained cell voltage at (a)C/2, (b) 1C, (b) 2C, and (c) 3C-discharge.	112
5.9	Variation of the surface temperature of the Samsung 18650 cell for (a) C/2, (b) 1C, (c) 2C and (c) 3C-discharge.	113
5.10	Different sources of heat generation in the cell for (a) C/2, (b) 1C, (c) 2C and (c) 3C-discharge current.	114

List of Tables

2.1	Governing equations of various thermal models	39
2.2	Various models implemented to analyze the performance of large format cells .	45
3.1	Parameters used for simulation of lithium-ion cell	63
3.2	RMSE in voltage for the proposed model, SPM2 and SPM under constant current discharge from 4.2 V to 3 V.	71
3.3	Simulation time for the proposed model, SPM2, SPM and P2D model under constant current discharge from 4.2 V to 3 V.	76
4.1	Species and charge conservation equations of pseudo-2D model.	82
4.2	Thermal parameters used for simulation of lithium-ion cell	88
4.3	Percentage and total heat generated for different discharge rates within each cell component (Negative values indicate that heat is absorbed).	99
4.4	Percentage and total heat generated for different charge rates within each cell component (Negative values indicate that heat is absorbed).	100
5.1	Relative composition of nickel, manganese and cobalt obtained in different samples.	106

Nomenclature

Abbreviations

BMS	battery management system
CPE	constant phase element
DAE	differential algebraic equation
DMC	dimethyl carbonate
DMP	differential mechanical parameter
DTV	differential thermal voltametry
DV	differential voltage
ECM	equivalent-circuit model
EC	ethylene carbonate
EHM	equivalent-hydraulic model
EIS	electrochemical impedance spectroscopy
EV	electric vehicle
FDM	finite difference method
GA	genetic algorithm
GPR	Gaussian process regression
IC	incremental capacity
NLLS	non-linear least-square

OCP	open-circuit potential
P2D	pseudo-2D
PDE	partial differential equation
PSO	particle swarm optimization
RUL	remaining useful life
RVM	relevance vector machine
SEI	solid electrolyte interface
SoC	state-of-charge
SoH	state-of-health
SPM	single-particle model
SVM	support vector machine

Symbols

α_a, α_c	anodic/cathodic charge transfer coefficients
$\dot{q}_{\text{mix},j}$	rate of heat generation due to mixing per unit volume in an electrode i (W/m ³)
\dot{q}_g	rate of heat generation per unit volume (W/m ³)
$\epsilon_{e,i}$	electrolyte volume-fraction in electrode i
$\epsilon_{s,i}$	active material volume-fraction in electrode i
η_i	surface overpotential for lithium intercalation/deintercalation reaction in electrode i (V)
λ_i	thermal conductivity of domain i (W/m.K)
$\phi_{e,i}$	ionic potential in the electrolyte phase (V)

$\phi_{s,i}$	electrical potential in electrode i (V)
ρ_i	density of domain i (kg/m ³)
σ_i	electrical conductivity for electrode i (S/m)
$a_{s,i}$	specific interfacial area for an electrode i (m ² /m ³)
C_e	lithium concentration in the electrolyte (mol/m ³)
$C_{\max,i}$	maximum lithium concentration for an electrode i (mol/m ³)
$C_{p,i}$	lithium concentration in an electrode particle i (mol/m ³)
$c_{p,i}$	specific heat capacity of domain i (J/kg.K)
$C_{s,i}$	lithium concentration on the surface of electrode particle i (mol/m ³)
D_e	lithium diffusion coefficient in electrolyte (m ² /s)
$D_{s,i}$	lithium diffusion coefficient in electrode i (m ² /s)
$E_{a,i}$	activation energy for property i (J/mol)
F	Faraday's constant (C/mol)
H_{par}	total enthalpy stored in electrode particle i (J)
$H_{v,j}$	enthalpy per unit volume in an electrode i (J/m ³)
I_{app}	applied current(A/m ²)
$i_{0,j}$	exchange current density for lithium intercalation/deintercalation reaction at electrode j (A/m ² .s)
$j_{0,i}$	exchange molar flux density for lithium intercalation/deintercalation reaction at electrode i (mol/m ² .s)

$j_{f,i}$	interfacial molar flux density for lithium intercalation/deintercalation reaction at electrode i (mol/m ² .s)
k	rate constant for lithium intercalation/deintercalation reaction (m ² /s)
L_i	thickness of cell component i (m)
R	universal gas constant (J/mol.K)
$R_{s,i}$	particle size for electrode i (m)
T	temperature (K)
t	time (s)
T_{amb}	ambient temperature (K)
t_+^0	cation transfer coefficient
$U_{H,i}$	enthalpy potential for electrode i (V)
U_i	open-circuit potential in electrode i (V)
V	cell voltage (V)
y_i	state-of-charge in electrode i

Subscripts

e	electrolyte
n	negative electrode
p	positive electrode
s	separator
ref	reference value

Superscripts

0 initial condition
avg average value
eff effective property